DOI: 10.4408/IJEGE.2013-06.B-16

THERMO-HYDRO-MECHANICAL ANALYSIS FOR THE SIMULATION OF RAPID SLIDING PROCESS IN A NEW AND FAST RING SHEAR PROTOTYPE

VICTOR SERRI, ENRIQUE ROMERO, ANTONIO LLORET, JOSEP SURIOL & EDUARDO E. ALONSO

Universitat Politècnica de Catalunya - Department of Geotechnical Engineering and Geosciences
Campus Nord UPC, Building D2 c/ Jordi Girona 1-3 - 08034 Barcelona, Spain

ABSTRACT

Vajont was a case of an extremely fast landslide and efforts to clarify the failure have been mainly concentrated in providing a consistent explanation taking into account this characteristic feature. Particularly in the case of Vajont landslide, attention has been essentially focused on the shearing properties of the sliding surface. An accepted explanation for the velocity reached is the thermo-hydraulic-mechanical coupling under saturated conditions, which induces thermal dilation and effective stress reduction due to pore pressure build-up. Nevertheless, lack of in situ and experimental information has become one of the main drawbacks when trying to explain these coupled processes. In situ information is difficult to obtain since temperature and pore pressure development during these fast processes are impossible of being measured. To overcome this limitation, a new fast sliding prototype -emulating a ring shear apparatus- has been recently developed at the Universitat Politècnica de Catalunya (Spain). This prototype can reach relatively high speeds along the sliding surface (up to 30 km/h) under relatively high total vertical stresses (up to 3 MPa). Temperature and pore pressure changes can be locally measured with miniature transducers located close to the shear band. The design of this complex prototype requires the use of simulation-aided techniques, to help with the interpretation of the coupled processes, as well as to estimate the maximum temperature and pore pressure changes. A thermo-hydro-mechanical formulation, applied to the ring shear test, is proposed in the paper to study pore water pressure build up and dissipation in a sliding surface being heated by the frictional work induced by the motion. Particularly, the proposed model is applied to simulate the evolution of the shear strength along the sliding surface during a fast sliding process.

KEY WORDS: *thermo-hydro-mechanical analysis, fast landslide, fast sliding ring shear apparatus*

INTRODUCTION

If a planar slide loses the conditions for strict equilibrium an accelerated motion will start. A simple dynamic calculation involving a rigid block sliding on an inclined base shows that, if the equilibrium is barely lost (i.e., the driving force exceeds the resisting one by a small amount), the increase of sliding velocity develops at a relatively slow rate. Some case records indicate, however, that very high velocities may develop in relatively short sliding distances.

For fast sliding, the case of Vajont is an important reference. The failure surface had an "open L" shape, which made even more difficult to explain why it reached such a high sliding velocity (about 100 km/h) in no more than 30 s (HENDRON & PATTON, 1985). In this case, the recorded slide motions in the last few months indicated equilibrium conditions were close to the critical ones (NONVEILLER, 1987). Basically, relatively small changes in pore water

pressures acting on the sliding surface led probably to a reduction of the shear strength of the soil, and as a consequence, to the acceleration of the sliding motion. Heat-induced pore water pressure rise on the sliding band, as suggested by (Voight & Faust, 1982), has been also considered as a tentative mechanism leading to the rapid sliding motion of Vajont (Vardoulakis, 2002; Alonso & Pinyol, 2010; Pinyol & Alonso, 2010). A similar mechanism has been also considered by (Rice *et alii,* 2010; Rice, 2006) to explain the reduction in the shear strength of faults as a result of fast earthquake slippage. Nevertheless, lack of in situ and experimental information has become one of the main limitations when trying to explain these coupled processes in fast landslides.

To get further experimental insight into these processes, a new fast sliding prototype has been recently developed at the Universitat Politècnica de Catalunya (Spain). The prototype was designed maintaining the annular shape of a ring shear apparatus and incorporating electronic control of torque and speed to emulate force and displacement control conditions. Numerical simulation tools were used to better understand the thermo-hydro-mechanical processes occurring at the sliding surface and design the prototype. Particularly, the present paper presents the formulation used in these highly coupled processes, which involve pore water pressure generation and dissipation in a shear band being heated by the frictional work induced by the sliding motion. Information on

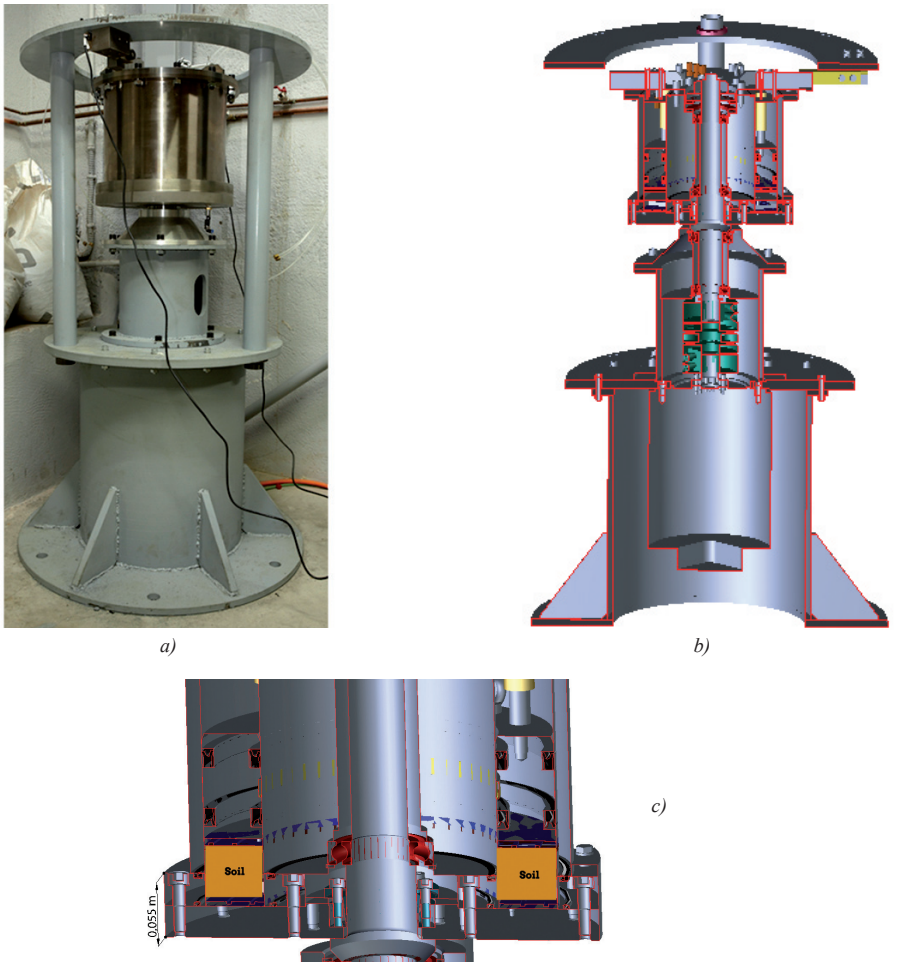

Fig. 1 - New fast ring shear apparatus a) Photograph of the new prototype (metallic plate at the base 350 mm in diameter); b) Cross-section of the apparatus; c) Zoom of the annular sample

maximum pore pressure build-up and its dissipation, as well as temperature increase and its dissipation, are key data for a better selection of transducers, their location and their time response along these fast processes. The paper presents a simulation of the pore pressure, temperature and shear strength evolutions along the sliding surface of a synthetic fast sliding test carried out on a low permeability material and with the same geometry of the prototype.

FAST RING SHEAR PROTOTYPE

The ring shear apparatus has been widely used in the analysis of slope stability, as it provides the advantage of large shear displacements –the sample can be sheared at displacements of varying magnitude–, there is no change in the area of the shear surface as the test runs, and that fast rotations can be easily implemented. The prototype developed at the Universitat Politècnica de Catalunya was based on the geometry of the cell proposed by (Bishop *et alii,* 1971) and enhanced - for fast landslides triggered by earthquake - by (Sassa *et alii,* 2004). To avoid the problems due to high centrifugal forces, the movable bottom part involved a small mass of soil just to ensure the sliding surface (Bromhead, 1979). A specially adapted o-ring ensured the waterproof condition of the cell (no radial flow condition along the sliding surface). The equipment includes an electronic control of torque or speed, which can reach relatively high velocities along the sliding surface (up to 30 km/h) under high total vertical stresses (up to 3 MPa). Total vertical stresses (applied through an upper piston) and pore pressures are also automatically controlled. Temperature and pore pressure changes can be fast and locally measured with miniature transducers located close to the shear band. Fig. 1 presents a photograph of the prototype, together with a cross-section and a zoom of the sample holder. The main characteristics of the equipment are summarised in Tab. 1.

Characteristics of the prototype		Values
Sample geometry	Outer diameter	300 mm
	Inner diameter	200 mm
	Maximum height	80 mm
	Minimum height	40 mm
Control characteristics	Maximum vertical stress	3 MPa
	Maximum torque	810 Nm
	Maximum velocity	30 km/h
	Velocity controlled	yes
	Torque controlled	yes
Temperature sensors	Number of sensors	6
	Range	< 300°C
	Resolution	0.15°C
Pressure sensor	Number of sensors	6
	Range	3 MPa
	Resolution	3 kPa
Force sensors	Number of sensors	2
	Range	500 kN
	Resolution	0.5 kN
Displacement sensor	Number of sensors (LVDT)	1
	Range	10 mm
	Resolution	< 0.010 mm

Tab. 1 Characteristics of the new fast ring shear prototype

GOVERNING THERMO-HYDRO-MECHANICAL EQUATIONS

Geometrical conditions are axisymmetric (annular sample shown in Fig. 2a). The problem has been simplified by considering the 2D section shown in Fig. 2b and 2c, which allows following an equivalent formulation to that described in (Pinyol & Alonso, 2010). The 2D section presents two main zones, separated by the sliding surface (shear band): a static one at the top and a movable one at the bottom (Fig. 2c).

Considering that in the sliding surface all the shear deformation is concentrated –the effective normal stress does not perform work–, the rate of work input into the band is given by

$$\dot{W} = \int_V \tau_f \dot{\gamma} dV \qquad (1)$$

where γ_f is the shear strength of the band material with volume V and $\gamma = v_{max}/2e$ the work conjugate (shear) strain rate ($2e$ is the band thickness and v_{max} the sliding velocity). It is important to remark that in the ring shear apparatus, the velocity depends on the radius. In this case, the velocity considered is the corresponding to the average radius. Assuming that all the work input has been converted totally into heat, it is possible to write

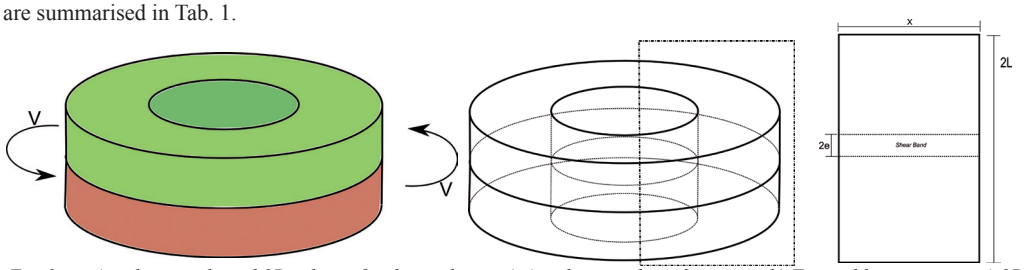

Fig. 2 - Annular sample and 2D scheme for the analyses: a) Annular sample and rotation, b) Top and bottom parts; c) 2D scheme (zoom of rectangle (b)

$$H(t) = \tau_f(t)\frac{v_{max}(t)}{2e} \quad (2)$$

where $H(t)$ is the heat generated by friction per unit volume and time t. The band increases its temperature as a consequence of this heating source, and pore water pressure in excess of that initially existing develops induced by thermal dilation of water. This pore water increase, which develops at relatively small elapsed times and under undrained conditions, reduces the shear strength of the band material.

Fig. 3 shows the rectangular domain and coordinates used. It represents half of the domain considered in Fig. 2c for symmetrical reasons (z axis directed normal to the band plane with origin located on the mid-plane of the shear band).

The excess pore pressure $u_w(x,z,t)$ –essentially caused by the thermal dilation of the water–, temperature $\theta(x,z,t)$, and velocity $v(z,t)$ are functions of the position in both directions (x,z) and time t. For example, the maximum excess pore pressure will be developed in the central plane of the shear band. Other assumptions are considered, such as full saturation of the porous medium and thermal conduction phenomena (soil and metallic walls of the cell).

As a summary, the set of equations governing the different thermo-hydro-mechanical processes are:

• Equilibrium conditions and Mohr Coulomb shear strength law

$$\tau_f(t) = (\sigma_n - p - u_w(t))tan\phi' \quad (3)$$

where σ_n is the normal (total) stress applied, p is the hydrostatic pore pressure, $u_w(t)$ is the excess pore pressure induced by heating due to soil friction and ϕ' is the angle of internal friction.

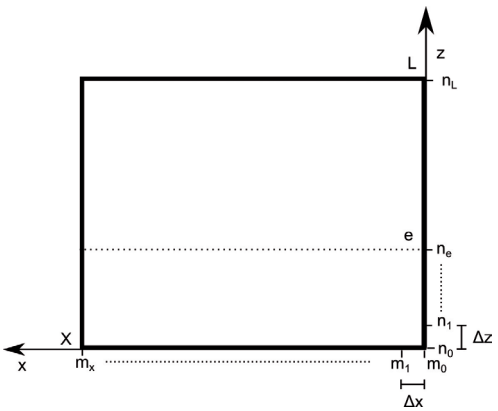

Fig. 3 - Discretisation used for modelling the 2D section. The domain is subdivided into n ΔXm small elements with the dimensions Δx and Δz

• First law of thermodynamics (shear band) given by Eq. (2).

• Heat balance

$$H = \rho c_m \frac{\partial\theta}{\partial t} - \Gamma\left(\frac{\partial^2\theta}{\partial x^2} + \frac{\partial^2\theta}{\partial z^2}\right) \quad (4)$$

where c_m is the specific heat of the saturated soil, ρ is the saturated soil density and Γ is the thermal conductivity coefficient.

• Mass balance (water and solid)

$$\begin{aligned}&[n\beta_w + (1-n)\beta_s]\frac{\partial\theta}{\partial t} + n\alpha_w\frac{\partial u_w}{\partial t} + \\ &- m_v\left(\frac{\partial\sigma_n}{\partial t} - \frac{\partial u_w}{\partial t}\right) + \\ &- \frac{1}{\gamma_w}\left(k_x\frac{\partial^2 u_w}{\partial x^2} + k_z\frac{\partial^2 u_w}{\partial z^2}\right) = 0\end{aligned} \quad (5)$$

where n is the porosity, β_w the thermal expansion coefficient of water, β_s the thermal expansion coefficient of solid, α_w the compressibility coefficient of water, m_v is the soil compressibility coefficient, γ_w the specific weight of water, and k_x and k_z the permeability in horizontal and vertical directions, respectively.

• Dynamic equilibrium

$$\frac{\partial v_{max}}{\partial t} = \frac{1}{M}\left(\tau_{unst} - \tau_f\right) \quad (6)$$

where τ_{uns} is the stress induced by the motor torque of the equipment that induces shearing and M is the mass involved in the movement.

To solve these equations it is also necessary to consider the initial and boundary conditions (the initial excess pore pressure and velocity are null at an initial room temperature).

NUMERICAL SOLUTION

The problem is solved using a numerical approximation. Applying the Taylor approximations, it is possible to write an explicit model. The step forward approximation is chosen. The derivative equations are written as

$$\begin{aligned}\frac{\partial f(x,z,t)}{\partial t} &= \frac{f|^{t+1}_{x,z} - f|^{t}_{x,z}}{\Delta t} \\ \frac{\partial^2 f(x,z,t)}{\partial z^2} &= \frac{f|^{t}_{x,z+1} - 2f|^{t}_{x,z} + f|^{t}_{x,z-1}}{\Delta z^2}\end{aligned} \quad (7)$$

Using the finite difference method, the heat and mass balance equations become

$$\begin{aligned}H = &\frac{\theta|^{t+1}_{x,z} - \theta|^{t}_{x,z}}{\Delta t}\rho c_m + \\ &+\Gamma\left(\frac{\theta|^{t}_{x,z+1} - 2\theta|^{t}_{x,z} + \theta|^{t}_{x,z-1}}{\Delta z^2} + \right. \\ &\left. + \frac{\theta|^{t}_{x+1,z} - 2\theta|^{t}_{x,z} + \theta|^{t}_{x-1,z}}{\Delta x^2}\right)\end{aligned} \quad (8)$$

$$[n\beta_w + (1-n)\beta_s]\frac{\theta|_{x,z}^{t+1} - \theta|_{x,z}^{t}}{\Delta t} + (n\alpha_w + m_v)\frac{u_w|_{x,z}^{t+1} - u_w|_{x,z}^{t}}{\Delta t} + -\frac{1}{\gamma_w}\left(k_x\frac{u_w|_{x+1,z}^{t} - 2u_w|_{x,z}^{t} + u_w|_{x-1,z}^{t}}{\Delta x^2} + k_z\frac{u_w|_{x,z+1}^{t} - 2u_w|_{x,z}^{t} + u_w|_{x,z+1}^{t}}{\Delta z^2}\right) = 0 \quad (9)$$

To obtain a stable solution, the Courant condition must be satisfied (Courant *et alii*, 1967)

$$\frac{k_x}{(m_v + n\alpha_w)\gamma_w}\frac{\Delta t}{\Delta x^2} + \frac{k_z}{\gamma_w}\frac{\Delta t}{\Delta z^2} \le 1 \quad (10)$$

To simplify the analysis, the permeability is considered the same in the two directions x and z. With the restriction indicated in Eq. (10), it is possible to obtain the interval Δt used in the numerical simulation.

SIMULATION RESULTS AND DISCUSSION

The parameters used in the simulation are summarised in Table 2. Thermal expansion coefficient, specific heat and compressibility coefficient for water and the solid particles were taken from (Olivella *et alii*. 1996). A soil thermal conductivity of 1.5 W m^{-1} K^{-1} has been considered according to (Lima *et alii,* 2009). Porosity and residual friction angle approximate the actual values of the Vajont sliding clay (Hendron & Patton, 1985). The initial temperature is 20ºC. A water permeability of 10^{-13} m/s for a high plasticity clay with low porosity has been considered for the base case (Lima *et alii*, 2009). Since no precise laboratory information on the water permeability is available, a complementary sensitivity analysis has been performed to study how the output of the numerical model is affected by the uncertainty of its value. The water permeability has been changed between 10^{-13} and 10^{-11} m/s (soils in the shear band and outside the band). A vertical stress of 100 kPa - not comparable with the real case of Vajont - has been used to show that even at low stresses these thermo-hydro-mechanical processes develop and have influence on the landslide movement.

Parameter	Symbol	Value
Water		
Density	ρ_w	1000 kg m^{-3}
Compressibility coefficient	α_w	$5\cdot10^{-10}$ Pa^{-1}
Thermal expansion coefficient	β_w	$2\cdot10^{-4}$ K^{-1}
Specific heat	c_w	$4.2\cdot10^{3}$ J kg^{-1} K^{-1}
Solid particles		
Density	ρ_s	2700 kg m^{-3}
Thermal expansion coefficient	β_s	$3\cdot10^{-5}$ K^{-1}
Specific heat	c_s	$8.4\cdot10^{2}$ J kg^{-1} K^{-1}
Shear band material		
Porosity	n	0.2
Thermal conductivity (material outside the band)	Γ	1.5 W m^{-1} K^{-1}
Compressibility coefficient	m_v	$1.5\cdot10^{9}$ Pa^{-1}
Angle of internal friction	ϕ'	12º
Water permeability (material outside the band)	k_x=k_z	10^{-13} m s^{-1} (base case)

Tab. 2 - Parameters used in the simulation

The hypothesis considered in the simulations assumes no radial flow along the sliding plane, which is consistent with the setup of the experimental prototype ('o-ring' between movable base plate and fixed top cap). On regarding lateral heat dissipation, simulations carried out by the authors have evidenced small lateral heat flows –compared to the heat generated- as a consequence of the fast processes involved (around 30 s).

Results for the base case with water permeability 10^{-13} m/s for both shear band and sliding mass are summarised in Fig. 4.

The evolution of the following variables has been plotted along time: excess pore water pressure and temperature generated in the shear band, shear strength, as well as sliding displacement and velocity. Some variables have been plotted in logscale to highlight the velocity increase with time and the consequent accelerated motion undergone by the slide at small elapsed times, as well as the heat generated even at small displacements. As observed in the figure, a key point in the simulation is the selection of the shear band thickness, since heat is generated in the band and not outside. Three different shear band thickness have been selected to perform the dynamic analyses reported here (*2e* represents the thickness), following the approach by (Vardoulakis, 2000): *e=0.5* mm, similar to the proposed by (Morgenstern & Tchalenko, 1967; Vardoulakis, 2001; Alonso & Pinyol, 2010) for clayey materials, *e=5* mm and *e=50* mm. For instance, (Vardoulakis 2001) proposes a thickness of 200 D_{50} for clays (i.e., 2 mm for D_{50}=0.01 mm). The code has been stopped at 500 m of horizontal displacement, which is equivalent to 100 revolutions in the ring shear cell.

In the case of *e=50* mm and during the first 10 s, the generated heat due to frictional work is not enough to increase the pore water pressure. This is a consequence of the large band thickness. Nevertheless, as the sliding mass undergoes acceleration (velocity increase), pore pressure build-up is able to decrease the shear strength due to vertical effective stress reduction. The shear strength reduces to a minimum value at elapsed times larger than 25 s. The effect of reducing the thickness of the band is observed in the figure, in which a clear increase of the velocity is detected from the beginning. For *e*=0.5 and 5 mm, the shear strength is reduced to a minimum at elapsed times around 10 s. These results agree well with data

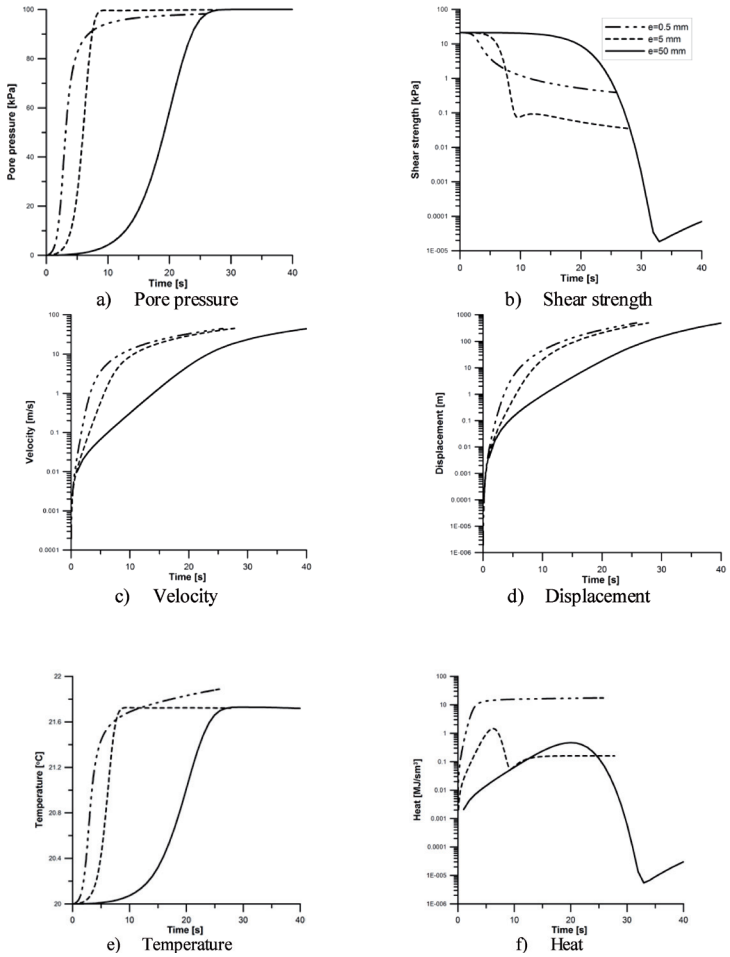

Fig. 4 - Simulation results for different shear band thickness with shear band permeability 10-13 m/s equal to the surrounding clay (base case)

reported by (Hendron & Patton 1985, Alonso & Pinyol 2010). These fast processes require miniature and fast response pressure and temperature transducers, which should be placed as close as possible to the sliding surface without interfering with the motion of the bottom sliding end of the prototype. The simulations of changing the water permeability between 10^{-13} and 10^{-11} m/s of the shear band and the surrounding clay indicate that essentially the same response is obtained as in the base case.

SUMMARY AND CONCLUSIONS

A new experimental apparatus - maintaining the annular shape of the ring shear - has been designed and constructed to study fast sliding processes promoted by heat induced friction. This mechanism has been an accepted explanation for the high velocity reached in the case of Vajont landslide. The prototype can reach high velocity along the sliding surface (up to 30 km/h and of the order of magnitude of the Vajont case) under relatively high total vertical stresses (up to 3 MPa). The design of this complex prototype requires the use of simulation-aided techniques to help with the interpretation of the thermo-hydro-mechanical coupled processes, which involve pore water pressure generation and dissipation in the shear band being heated. The paper presented the coupled formulation, the numerical solution adopted and the simplified geometry used for the equipment. The numerical results reported that shear strength vanishes at elapsed times around 10 s for

relatively small shear band thickness (below 10 mm) and low permeability (between 10^{-13} and 10^{-11} m/s). These synthetic results are used to better know the location, range, sensitivity and fast response required for the temperature and pressure transducers, which are located close to the sliding surface.

ACKNOWLEDGMENTS

The authors acknowledge the financial support provided by BIA2008-06614 research project of the 'Subdirección General de Proyectos de Investigación' (Ministerio de Economía y Competitividad, Spain).

REFERENCES

Alonso E.E. & Pinyol N.M. (2010) - *Criteria for rapid sliding I. A review of Vaiont case.* Engineering Geology, **114** (3-4): 198-210.

Bishop A.W.,Green G.E.,Garga V.K.,Brown J.D. & Andersen A. (1971) - *A new ring shear apparatus and its application to the measurement of residual strength*. Géotechnique, **21** (4): 273-328.

Bromhead E.N. (1979) - *A simple ring shear apparatus.* Ground Engineering, **25** (5): 40-44.

Courant R., Friedrichs K. & Lewy H. (1967) - *On the partial difference equations of mathematical physics*. IBM Journal of Research and Development, **11** (2): 215-234.

Hendron A.J. & Patton F. D. (1985) - *The Vaiont Slide, a geotecinical analysis based on new geologic observations of the failure surface.* Technical Report GL-85-5. Department of the Army US Army Corps of Engineers, Washington, DC.

Lima A., Romero E, Vaunat J., Gens A. & Li X. (2011) - *Heating pulse tests under constant volume on natural Boom clay. Experimental results and numerical simulations.* TIMODAZ Conf. 2009: Impact of thermo-hydro-mechanical-chemical (THMC) processes on the safety of underground radioactive waste repositories, 1-6.

Morgenstern N.R. & Tchalenko J.S. (1967) - *Microscopic structures in kaolin subjected to direct shear.* Geotechnique, **14** (4): 309-328.

Nonveiller E. (1987) - *The Vajont reservoir slope failure.* Engineering Geology, **24** (1-4): 493-512.

Olivella S., Gens A., Carrera J. & Alonso E.E. (1996) - *Numerical formulation for a simulator (CODE_BRIGHT) for the coupled analysis of saline media.* Engineering Computations, **21**(7): 87-112.

Pinyol N.M. & Alonso E.E. (2010) - *Fast planar slides. A closed-form thermo-hydro-mechanical solution.* International Journal for Numerical and Analytical Methods in Geomechanics, **34**(1): 27–52.

Rice J.R. (2006) - *Heating and weakening of faults during earthquake slip.* Journal of Geophysical Research, **111** (B5): 1-30.

Rice J.R., Dunham E. M. & Noda Y. (2010) - *Thermo-and hydro-mechanical processes along faults during rapid slip.* Engineering **85**(1978): 3-16.

Sassa K., Fukuoka H., Wang G. & Ishikawa N. (2004) - *Undrained dynamic-loading ring-shear apparatus and its application to landslide dynamics.* Landslides, **1**: 7-19.

Vardoulakis I. (2000) - *Catastrophic landslides due to frictional heating of the failure plane.* Mechanics of Cohesive frictional Materials, **5** (6): 443-467.

Vardoulakis I. (2001) - *Thermo-poro-mechanics of rapid fault shearing. In continuous and discontinuous modelling of cohesive*. Vermeer P., Herrmann H., Luding S., Ehlers W., Diebels S. & Ramm E. (eds.). Springer Berlin / Heidelberg, 63-74.

Vardoulakis I. (2002) - *Steady shear and thermal run-away in clayey gouges*. International Journal of Solids and Structures, **39** (13-14): 3831-3844.

Voight B. & Faust C. (1982) - *Frictional heat and strength loss in some rapid landslides*. Géotechnique, **32**(1): 43-54

